microbial biotechnology

Infection and distribution of *Candidatus* Liberibacter asiaticus in citrus plants and psyllid vectors at the cellular level

Qian Chen* (iD) Zhiqiang Li, Shulin Liu, Yunhua Chi, Dongsheng Jia and Taiyun Wei
Vector-borne Virus Research Center, Fujian Province Key Laboratory of Plant Virology, Institute of Plant Virology, Fujian Agriculture and Forestry University, Fuzhou, Fujian, 350002, China.

Summary

Huanglongbing (HLB) is currently considered the most destructive disease of citrus worldwide. In the major citrus-growing areas in Asia and the US, the major causal agent of HLB is the bacterial pathogen *Candidatus* Liberibacter asiaticus (CLas). CLas is vectored by the Asian citrus psyllid, *Diaphorina citri*, in a persistent propagative manner. CLas cannot be cultured *in vitro* because of its unclear growth factors, leading to uncertainty in the infection mechanism of CLas at the cellular level in citrus and in *D. citri*. To characterize the detailed infection of CLas in the host and vector, the incidence of HLB was first investigated in citrus-growing fields in Fujian Province, China. It was found that the positive association of the level of CLas infection in the leaves correlated with the symptoms. Then antibodies against peptides of the outer membrane protein (OMP) of CLas were prepared and tested. The antibodies OMP-225, OMP-333 and OMP724 showed specificity to citrus plants in western blot analyses, whereas the antibodies OMP-47 and OMP-225 displayed specificity to the *D. citri* vector. The application of OMP-225 in the immunofluorescence assay *indicated* that CLas was located in and distributed throughout the phloem sieve cells of the leaf midribs and axile placenta of the fruit. CLas also infected the epithelial cells and visceral muscles of the alimentary canal of *D. citri*. The application of OMP-333 in immunoelectron microscopy indicated the round or oval CLas in the sieve cells of leaf midribs and axile placenta of fruit as well as in the epithelial cells and

reticular tissue of *D. citri* alimentary canal. These results provide a reliable means for HLB detection, and enlighten a strategy via neutralizing OMP to control HLB. These findings also provide insight for the further investigation on CLas infection and pathogenesis, as well as CLas–vector interaction.

Introduction

Citrus huanglongbing (HLB), also known as citrus greening disease, is currently devastating the citrus industry worldwide (Gottwald, 2010). HLB produces a chronic infection that causes tree decline, even death and some plants will never produce usable fruit (Halbert and Manjunath, 2004). HLB causes leaf yellowing and blotchy mottling, which are the most characteristic symptoms of HLB (Dala-Paula *et al.*, 2018; Zheng *et al.*, 2018). HLB also causes fruit to be small, lopsided and misshapen. Some fruits turn from green to yellow or orange in the peduncular end, while the stylar end remains green (Dala-Paula *et al.*, 2018). Due to the absence of a treatment for HLB, the worldwide citrus industry is susceptible to HLB. Current disease control mainly involves a combination of approaches including the control of the transmission pathway and control of the causal agent (Bove, 2006; Wu *et al.*, 2018). The presumed pathogen of HLB is a Gram-negative and phloem-limited bacterium, and there are three species, *Candidatus* Liberibacter asiaticus (CLas), *Ca*. Liberibacter africanus (CLaf) and *Ca*. Liberibacter americanus (CLam) based on the 16S rDNA (Jagoueix *et al.*, 1997; Hocquellet *et al.*, 1999; Sagaram *et al.*, 2009). In the major citrus-growing areas in Asia and the US, CLas is the major causal agent of HLB (Clark *et al.*, 2018).

In nature, CLas is mainly vectored in a persistent and propagative manner by the Asian citrus psyllid, *Diaphorina citri* Kuwayama (Hemiptera: Liviidae), which is the most important transmission pathway of CLas (Ammar *et al.*, 2016). Nymphs and adults of *D. citri* can acquire CLas at least 30 min after feeding, and the ability of nymphs to acquire CLas is higher than that of the adults (Hung *et al.*, 2004; Ammar *et al.*, 2016). CLas can systemically infect *D. citri* organs, including salivary glands, filter chamber, fat bodies, alimentary canal and reproductive organs (Ammar *et al.*, 2011; Grafton-Cardwell *et al.*, 2013).

Currently, CLas cannot be cultured *in vitro* due to its unclear growth factors. The continuous axenic culture of CLas has been particularly challenging and very limited success has been achieved, though many research groups are working on exploring conditions suitable for CLas culture *in vitro* (Sechler *et al.*, 2009; Parker *et al.*, 2014; Merfa *et al.*, 2019). The lack of a mature system for sustained axenic culture of CLas *in vitro* and few techniques for CLas enrichment have restricted the confirmation of the morphology of CLas. To date, the investigation on the morphology of CLas is based only on electron microscopy of the phloem of the plant host or organs of *D. citri*. Shokrollah *et al.* (2010) reported that CLas is a spherical or rod-shaped particle with a length ranging from 594.57 to 1368.16 nm and width ranging from 201.68 to 811.15 nm. Hilf *et al.* (2013) characterized CLas as a pleiomorphic round and elongated bacilliform-like shape, which has a size of 0.30 to 0.99 μm. Another previous study reported that CLas-resembling structures are rod-shaped, varying from 0.39 to 0.67 μm long and 0.19 to 0.39 μm wide and spherical-shaped ranging from 0.61 to 0.80 μm in diameter (Mann *et al.*, 2011). These observations show inconsistency with each other due to the lack of use of immunoelectron microscopy (iTEM) in these previous studies.

The outer membrane protein (OMP), located in the bacterial outer membrane, functions in the bacterial life cycle, including the establishment of bacterial structure, induction of bacterial immune response, regulation of bacterial adaptation, initiation of the bacteria–host interaction, activation of host immune response and so on (Lin *et al.*, 2002; Bishop, 2008). In addition, different plant varieties cause different mutations of the OMP (Bastianel *et al.*, 2005). The OMP also possesses immunogenicity and is a suitable antigenic protein for the preparation of antibodies. Therefore, the OMP serves as a preferred target for bacterial control. The polyclonal antibody against the major outer membrane protein (OMPA) of CLas can be used to blot CLas in phloem tissue (Ding *et al.*, 2015, 2016, 2017); however, these tissue blots could not clarify the distribution of CLas at the cellular level in citrus plants and *D. citri* vectors.

Here, we aimed to determine a specific antibody against an OMP to trace the infection of CLas in the citrus host and *D. citri* vector at the cellular level, which can be used to establish an elaborate system for CLas detection. We prepared several antibodies against peptides of CLas OMP and their specificity was determined via western blot, immunofluorescence assays and iTEM. The morphology and the infection of CLas in citrus hosts and *D. citri* vectors were characterized. The results provide a reliable means for HLB detection. In addition, our results provide valuable insights into the mechanism of CLas infection and pathogenesis, as well as plant–CLas–insect interaction.

Results

Survey of citrus-growing fields for HLB incidence

We first investigated the incidence of HLB in citrus-growing fields in Fujian Province, China. The citrus plants cultivated in the field included tangelo (*C. paradisi*×*C. tangerine*), *C. poonensis* Hort. ex Tanaka, *C. reticulata* Blanco cv. Aiyuan 38, *C. reticulata* Blanco cv. Tangerine, *C. sinensis* var. *brasiliensis* Tanaka, *C. reticulata* Blanco cv. Fertile orange, Shatang ju and *C. grandis* Osbeck cv. Pomelo. We found that in some citrus-growing fields, citrus plants displayed yellow colouration, asymmetrical yellowing, blotchy mottling on leaves and delayed flowering (Fig. 1A). Some diseased fruit changed colour from the stem downward, while healthy fruit changed colour from bottom upward (Fig. 1A). *D. citri* could be found on the flush tips or on the abaxial leaf surface of the citrus plants (Fig. 1A). Samples suspected to be diseased, including leaves, flowers, and fruits, as well as *D. citri* vectors, were collected.

The total DNA was extracted from these samples for PCR, with the primers specific for 16S rDNA gene. The PCR products that were consistent with the expected size were recovered for sequencing. Based on the sequencing results, the samples that had correct sequences of the 16S rDNA gene were determined to be infected with CLas. The results showed that some leaves, flowers and fruit were infected with CLas. The positive rate of leaves ranged from 17.0% to 48.1% (Table 1). The infection rate of *D. citri* vectors ranged from 28.3% to 41.6% (Table 2). These results indicated that citrus plants and *D. citri* vectors were infected to different degrees at different locations of Fujian Province (Fig. 1B), which provided basic data for downstream

Fig. 1. The survey of HLB incidence in citrus-growing fields in Fujian Province, China.
A. The symptoms of HLB in the whole plants, leaves, fruit (I–IV), and *D. citri* on diseased plants (V–VII) in the fields we sampled. White arrows indicate *D. citri* vectors.
B. The occurrence of HLB in citrus-growing fields in Fujian Province. The leaves or fruit showing HLB symptoms were sampled and individually assayed. The incidence of HLB was determined by PCR tests for 16S rDNA of CLas and the HLB incidence is shown on the map of Fujian Province. White arrows indicate *D. citri* vectors.
C. The qPCR analysis of the CLas titres in the symptomatic and asymptomatic leaves of symptomatic or asymptomatic plants. (I) The sampled location and symptom of tested leaves. (II) CLas titres in the leaves of Tangelo (*C. paradisi*×*C. tangerine*) sampled at Fuqing and *C. sinensis* var. *brasiliensis* Tanaka sampled at Gutian. +, symptomatic. -, asymptomatic. *$P < 0.05$. **$P < 0.01$. ***$P < 0.001$. ****$P < 0.0001$.
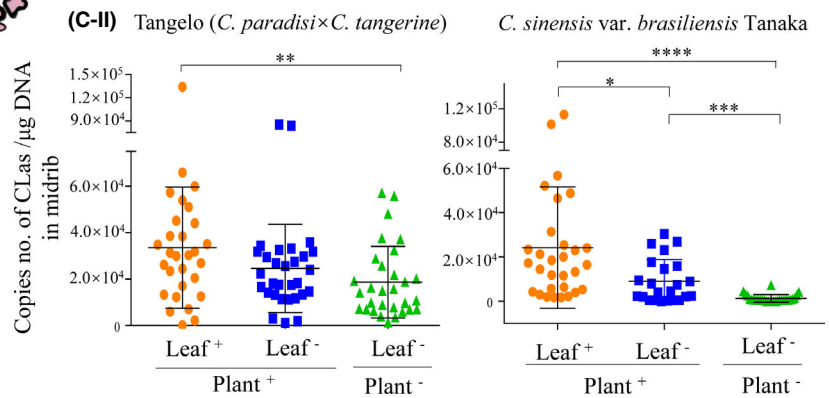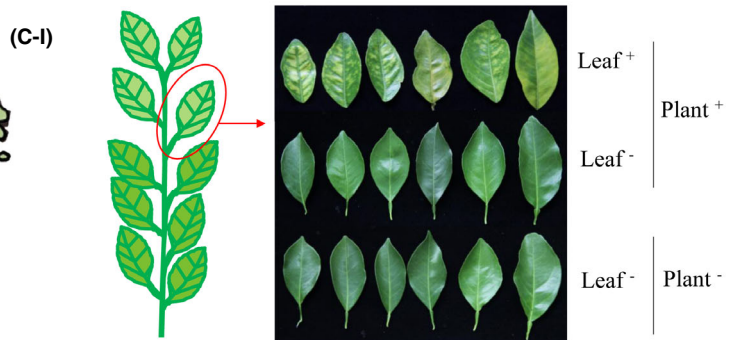
Table 1. The HLB incidence in citrus plants in Fujian Province, China via PCR tests using DNA from leaf midribs.

Location	Citrus variety	No. of samples	CLas-positive rate (%)
Fuqing	Tangelo (*C. paradisi*× *C. tangerine*)	16	43.8 (4/16)
Shunchang	*C. poonensis* Hort. ex Tanaka *C. reticulata* Blanco cv. Tangerine	55	34.5 (19/55)
Gutian	*C. sinensis* var. *brasiliensis* Tanaka	27	48.1 (13/27)
Fuan	*C. sinensis* var. *brasiliensis* Tanaka	30	16.7 (5/30)
Longyan	*C. reticulata* Blanco cv. Fertile orange *C. poonensis* Hort. ex Tanaka	5	60.0 (3/5)
Xiapu	*C. grandis* Osbeck cv. Pomelo	25	36.0 (9/25)

Table 2. CLas infection in *D. citri* populations in Fujian Province.

Location	No. of samples	CLas-positive rate (%)
Fuqing	34	29.4 (10/34)
Shunchang	60	28.3 (17/60)
Gutian	185	41.6 (77/185)

disease control and experimental materials for further investigation.

To understand the association of HLB symptoms with the level of CLas infection, new leaves close to the tips were sampled from citrus-growing fields at Gutian and Fuqing, respectively. These leaves were then classified into three types: symptomatic leaves of symptomatic plants, asymptomatic leaves of symptomatic plants and asymptomatic leaves of asymptomatic plants (Fig. 1C). The CLas titres in the midribs of these leaves were examined using qPCR assays. The results showed that in the Tangelo (*C. paradisi*×*C. tangerine*) samples from Fuqing, the mean of CLas titres in the midribs of symptomatic leaves of symptomatic plants was 3.36×10^4 copies / μg DNA (Fig. 1C; Table S1). These data were significantly higher than the titres from asymptomatic leaves of asymptomatic plants, which were 1.87×10^4

copies μg DNA^{-1}. The titres from asymptomatic leaves of symptomatic plants were 2.46×10^4 copies / μg DNA (Fig. 1C; Table S1), which was not significant compared with those of the symptomatic leaves of symptomatic plants and the asymptomatic leaves of asymptomatic plants. The results of *C. sinensis* var. *brasiliensis* Tanaka samples from Gutian showed that the mean of CLas titres in the midribs of symptomatic leaves of symptomatic plants was 2.42×10^4 copies / μg DNA, which was significantly higher than those of the asymptomatic leaves of symptomatic plants and the asymptomatic leaves of asymptomatic plants (Fig. 1C; Table S1). The mean titres from the asymptomatic leaves of symptomatic plants which was 9.04×10^4 copies / μg DNA, was significantly higher than that of the asymptomatic leaves of asymptomatic plants that was 1.29×10^3 copies / μg DNA (Fig. 1C; Table S1). These results indicate the positive association of CLas infection levels with leaf symptoms.

The specificity of antibodies against OMP

To understand the infection of CLas in citrus plants and *D. citri* vectors, we prepared the specific antibodies against OMP. The full length of the OMP gene (GenBank accession number KC473155) is 2346 bp and it encodes a protein containing 781 amino acids. The weight of the predicted OMP is approximately 87 kDa. The prediction analysis did not show the presence of signal peptide cleavage sites in the amino acid sequence (Fig. S1A). A transmembrane region was predicted between 1 and 100 aa (Fig. S1B). Combined with the analyses of hydrophilicity and antigenicity, nine regions were chosen for peptide synthesis for antibody preparation (Fig. 2A).

The polyclonal antibodies were purified and tested for specificity using a western blot assay. The prokaryotic-expressed OMP proteins first served as antigens. The results showed that the antibodies against peptides at 47–61 aa, 225–238 aa, 333–347 aa and 724–738 aa, which were named OMP-47, OMP-225, OMP-333 and OMP-724, respectively, could recognize an 87-kDa protein, consistent with the predicted molecular weight of OMP. OMP-47, OMP-225, OMP-333 and OMP-724 showed different degrees of specificity for prokaryotic-expressed OMP protein. The total protein extracted from

**Fig. 2.** Specificity of antibodies against OMP peptides.
A. Schematic illustration of the peptide design of an 87-kDa OMP.
B. Western blot analyses showing specificity of antibodies of OMP-47, OMP-225, OMP-333, and OMP-724. Total proteins of *E. coli* strain Rosetta expressing OMP or empty vector (Mock), CLas-infected or healthy midribs, or CLas-infected or uninfected *D. citri* were separated by SDS-PAGE and analysed with these antibodies. Arrow heads indicate bands with correct molecular weight. Lane M, protein ladder. +, positive. -, negative.
C. Schematic illustration of PCR tests for midribs before western blot analyses. PCR assays were performed to determine the CLas presence in DNA extracted from one end of the midrib. Total protein extracted from another end of the CLas-positive midrib was tested for western blot assays.

CLas-infected midribs of *C. poonensis* Hort. ex Tanaka were used as samples, whereas the total protein extracted from uninfected midribs of citrus plants (*C. reticulata Blanco* cv. Shatangju) maintained in the laboratory served as controls (Fig. 2B and C). The results showed that OMP-333 and OMP-724 specifically
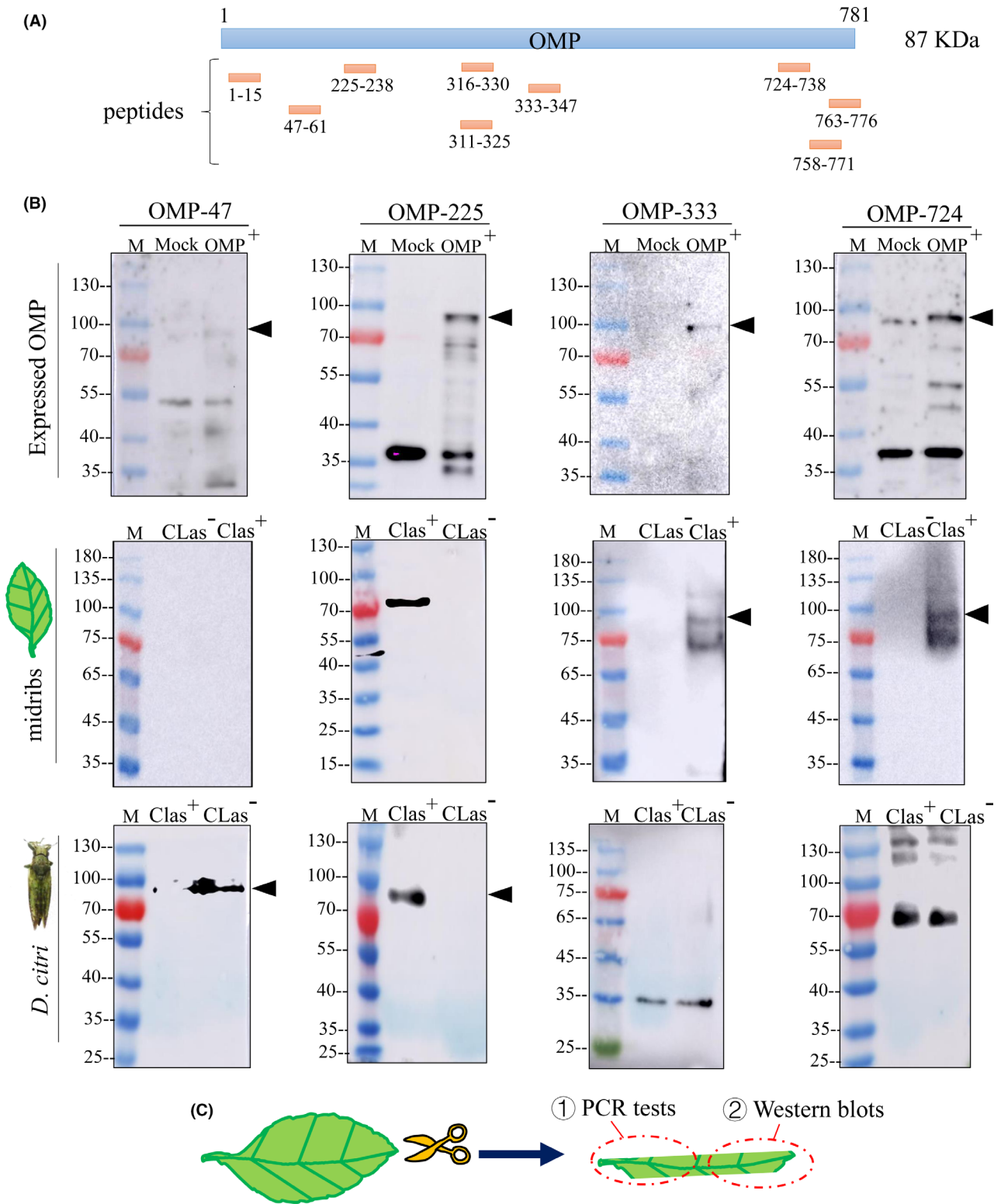
recognized 87-kDa OMP in CLas-infected midribs (Fig. 2B). The total protein extracted from *D. citri* collected from diseased citrus-growing fields were used as samples, whereas the total proteins extracted from uninfected *D. citri* were the controls. The results showed that OMP-47 and OMP-225 specifically recognized 87-kDa OMP in *D. citri* (Fig. 2B). Taken together, OMP-333 and OMP-724 were linear structural antibodies against OMP in citrus plants, and OMP-47 and OMP-225 were linear structural antibodies against OMP in *D. citri* vectors.

CLas located in the sieve cells of citrus plant phloem

The location of CLas in citrus plants *in vivo* was examined using the specific antibodies against OMP. The frozen sections of CLas-positive midribs derived from leaves collected from citrus fields in Fuqing, Gutian and Shunchang served as test samples (Fig. 3A). Those of CLas-negative midribs derived from leaves of uninfected citrus plants (*C. reticulata Blanco* cv. Shatangju), or from leaves of orange jessamine (*Murraya* Koenig ex Linn.) plants, served as negative controls (Fig. 3B). The immunofluorescence assays indicated that OMP-225 showed non-specific signals in the phloem of uninfected midribs of controls, but specifically immunolabelled the phloem of CLas-infected leaf midribs of *C. poonensis* Hort. ex Tanaka (Fig. 3B). Abundant OMP antigens accumulated in the sieve tubes that encircled the xylem (Fig. 3B). The association of concentration of CLas with symptoms was then tested in *C. sinensis* var. *brasiliensis* Tanaka using OMP-225. The immunofluorescence assays showed non-specific signals in the phloem of almost asymptomatic leaves of asymptomatic plants and showed strong signals in the phloem of most of the symptomatic leaves of symptomatic plants (Fig. 3C). In contrast, weaker signals were shown in the phloem of some asymptomatic leaves of symptomatic plants (Fig. 3C). Therefore, these results are consistent with those of the qPCR assays that also suggest a positive

relationship between the concentrations of CLas and leaf symptoms. iTEM was then performed to test the CLas-positive midribs (Fig. 3D). The uninfected midribs derived from the leaves of citrus plants or from the leaves of orange jessamine plants served as the negative control (Fig. 3E). The results demonstrated abnormal cellular structure in the sieve cells of CLas-infected midribs as well as the degeneration and decrease of organelles, including vacuoles, chloroplasts and mitochondria (Fig. 3E). The sieve cells of controls had homogeneous cytoplasm, intact organelles and clear cellular structures (Fig. 3E). The specificity of OMP-47, OMP-225, OMP-333, or OMP-724 was tested using iTEM. The antibodies of OMP-333 specifically immunolabelled the membrane of bacteria-like structures in sieve cells (Fig. 3E). These bacteria appeared round or oval, approximately 250–500 nm in diameter (Fig. 3E). In contrast, in the negative controls, no bacteria or colonies of bacteria were specifically immunolabelled (Fig. 3E). These results not only showed the specificity of OMP-333 in iTEM, but also displayed the distribution and morphology of CLas at the cellular level.

We also detected CLas in the diseased fruit of *C. poonensis* Hort. ex Tanaka that showed the symptom of colour inversion. The CLas-negative axile placenta of fruit from uninfected *C. reticulata Blanco* cv. Shatangju plants growing in the lab served as controls. The CLas-infected axis of diseased fruit and control samples were treated for frozen sectioning (Fig. 4A). Immunofluorescence assays showed that OMP-225 specifically immunolabelled the phloem of the axile placenta of diseased fruit, but specific immunolabelling was not observed in the controls (Fig. 4B). These results were consistent with those of the midribs and indicated that OMP-225 was a spatial structural antibody against OMP. OMP-225 could be applied for immunolabelling to study the location of CLas infection at the cellular level. In the control, the iTEM showed that the cytoplasm was homogeneous, the organelles were intact and the cellular structures were clear

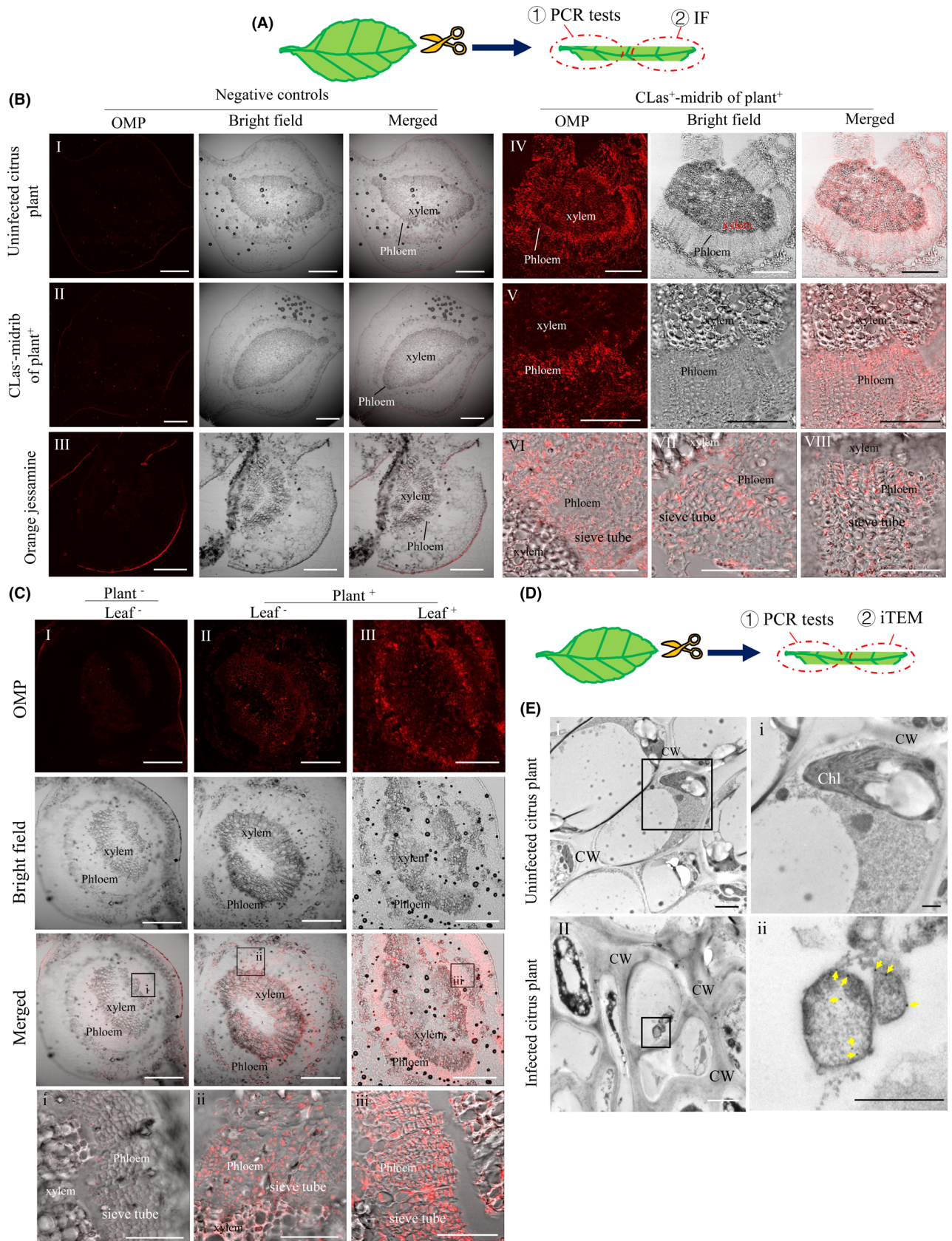**Fig. 3.** The localization and distribution of CLas in the phloem of midribs in citrus leaves.
A. Schematic illustration of midribs before immunofluorecence assays. PCR assays were first performed to determine the presence of CLas in DNA extracted from one end of the midrib. Then the other end of the CLas-positive midrib was sectioned for immunofluorecence assays. IF, immunofluorecense assays.
B. Immunofluorecence micrographs showing that OMP-225 specifically immunolabelled the phloem sieve cells in CLas-positive midribs. Sections of uninfected leaf midribs, CLas-negative leaf midribs of locally infected citrus plants and leaf midribs of orange jessamine plants, served as negative controls. The sections were immunostained with OMP-225-rhodamine. CLas⁻, CLas-negative. CLas⁺, CLas-positive. Plant⁺, symptomatic plant. Bars, 200 μm (I–IV), 100 μm (V) and 50 μm (VI–VIII).
C. Immunofluorecence micrographs showing strong signals in the phloem of most symptomatic leaves of symptomatic plants, and non-specific signals in the phloem of almost all of the asymptomatic leaves of asymptomatic plants. The images i, ii and iii are the enlarged image of the boxed area in images I, II and III. +, symptomatic. -, asymptomatic. Bars, 200 μm (I–III), 50 μm (i–iii).
D. Schematic illustration of midribs before iTEM. The PCR assay was first performed to determine the presence of CLas in DNA extracted from one end of the midrib. Then, the other end of the CLas-positive midrib was sectioned for iTEM.
E. Electron micrographs that show the immunogold labelling of OMP-333 on the membrane of round or oval CLas bacterium in sieve cells in leaf midribs of CLas-infected citrus. Yellow arrows indicate gold particles. The images i and ii are the enlarged image of the boxed area in images I and II. CW, cell wall. Chl, chloroplast, Bars, 2 μm (I and II), 600 nm (ii) and 500 nm (i).
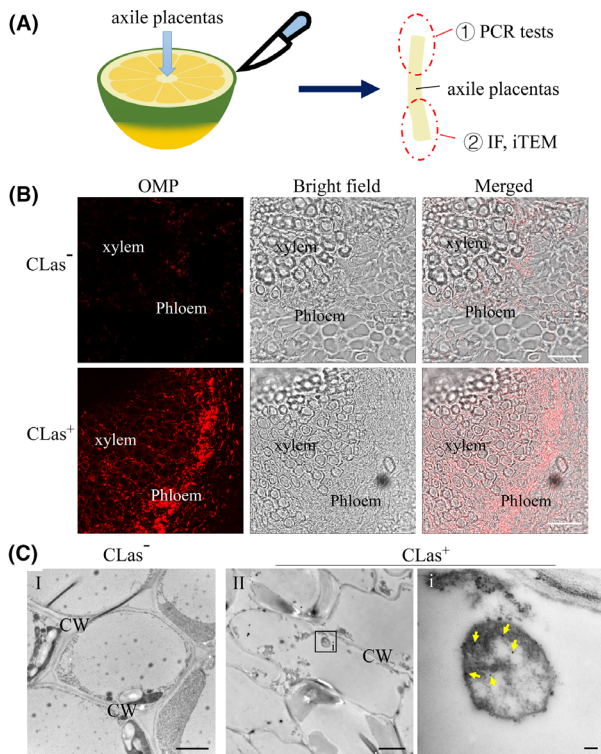
(A)

axile placentas

① PCR tests

axile placentas

② IF, iTEM

(B)

OMP   Bright field   Merged

CLas⁻   xylem / Phloem

CLas⁺   xylem / Phloem

(C)

CLas⁻   CLas⁺

I   CW   II   CW   i

Fig. 4. The localization and distribution of CLas in the phloem of the axile placenta of diseased fruit.
A. Schematic illustration of axile placenta before immunofluorescence and iTEM assays. The PCR assay was first performed to determine the presence of CLas in DNA extracted from one end of the axile placentas. Then, the other end of the CLas-positive axile placenta was treated for immunofluorescence and iTEM assays. IF, immunofluorescence assay.
B. Immunofluorescence microscopy showing that OMP-225 specifically immunolabelled the phloem sieve cells in CLas-positive axile placenta. The CLas-negative axile placenta of fruit from uninfected citrus plants served as a control. The sections were immunostained with the OMP-225-rhodamine. Bars, 50 μm.
C. The iTEM showing immunogold labelling of OMP-333 on the membrane of oval round CLas bacterium in sieve cells in CLas-positive axile placenta of disease fruit. The CLas-negative axile placenta of fruit from uninfected citrus plants served as a control. Yellow arrows indicate gold particles. The image i is the enlarged image of the boxed area in image II. CW, cell wall. Bars, 2 μm (I and II) and 100 nm (i). CLas⁻, CLas-negative. CLas⁺, CLas-positive.

(Fig. 4C). In contrast, infected axile placenta contained decreased organelles in the sieve cells that appeared unhealthy. OMP-333 in sieve cells specifically immunolabelled the membrane of round or oval bacterium that was approximately 250–500 nm in diameter. These results are also consistent with that observed in the midribs.

CLas accumulation in epithelial cells of D. citri alimentary canal

Next, the specificity of antibodies against OMP in *D. citri* vectors was tested and the accumulation of CLas was examined. The colony of *D. citri*, reared in the laboratory and separated from diseased plants, was determined to be CLas-negative before immunofluorescence assays and served as a control. *D. citri* collected from CLas-infected citrus plants were dissected and the alimentary canals were removed from bodies (Fig. 5A). The individual bodies of *D. citri* were first tested for the presence of CLas using PCR assays (Fig. 5A). Then, the alimentary canal of *D. citri*, of which bodies was CLas-positive, was treated for immunofluorescence assays (Fig. 5A). The *D. citri* alimentary canal containing the filter chamber, midgut and hindgut was composed of several epithelial cells and was covered by visceral muscle on the surface (Fig. 5B). Immunofluorescence assays showed that OMP-225 specifically immunolabelled the OMP antigens in epithelial cells in some CLas-positive *D. citri* alimentary canal, whereas the of alimentary canal of the control insects was not immunolabelled (Fig. 5B–G). These findings indicated that OMP-225 could be applied in *D. citri* in immunofluorescence assays. Then, we performed an immunofluorescence assay to examine the location of OMP to investigate the infection of CLas. CLas was distributed diffusely throughout the cytoplasm of epithelial cells of the anterior midgut, middle midgut and posterior midgut (Fig. 5C–E). The number of CLas-infected cells ranged from one to several, with up to approximately 50% of the epithelial cells of the alimentary canal infected (Fig. 5C–E). CLas could also infect the visceral

Fig. 5. The localization and distribution of CLas in the gut of the *D. citri* vector.
A. Schematic illustration of CLas infection before immunofluorescence and iTEM assays. The PCR assay was first performed to determine the presence of CLas in *D. citri* bodies. Then the gut of a CLas-positive individual was treated for immunofluorescence and iTEM assays.
B–G. Immunofluorescence microscopy showing CLas absence in the gut of healthy *D. citri* individuals (B) and accumulation in epithelia cells (C–E), visceral muscles (F), and even in the whole gut (G) in CLas-infected *D. citri*. Image B–I is a transmission light micrograph of the dissected gut of *D. citri*. The gut of *D. citri* was treated with OMP-225-rhodamine (red) and actin dye phalloidin-Alexa Fluor 647 carboxylic acid (blue), and examined by confocal microscopy. The images with red fluorescence (OMP-225-rhodamine) and blue fluorescence (actin dye) were merged. The images i, ii, and iii are the enlarged images of the boxed area in images C, D, and E. Es, oesophagus; FC, filter chamber; AMg, anterior midgut; MMg, middle midgut; PMg, posterior midgut; HG, hind gut; Mt, Malpighian tubule; EC, epithelial cell; CM, circular muscle; LM, longitudinal muscle. Bars, 200 μm (B and G–I), 100 μm (E, G–II), 50 μm (C, D, iii, F), and 20 μm (i and ii).
H. The qPCR analysis of the CLas titres in the *D. citri* bodies, of which the guts were immunofluorescence-positive significantly higher than those in *D. citri* bodies of which the guts were immunofluorescence-negative, tested with a qPCR assay. IF, immunofluorescence assays. **$P < 0.01$.
I and J. The iTEM showing absent detection of OMP-333 in the epithelia cells of the gut of healthy *D. citri* individuals (I) and immunogold labelling of OMP-333 on the membrane of oval or round CLas bacterium in the gut corresponding to CLas-positive bodies (J). The gut of CLas-negative *D. citri* served as a control. Yellow arrows indicate gold particles. CLas⁻, CLas-negative. CLas⁺, CLas-positive. Bars, 500 nm.
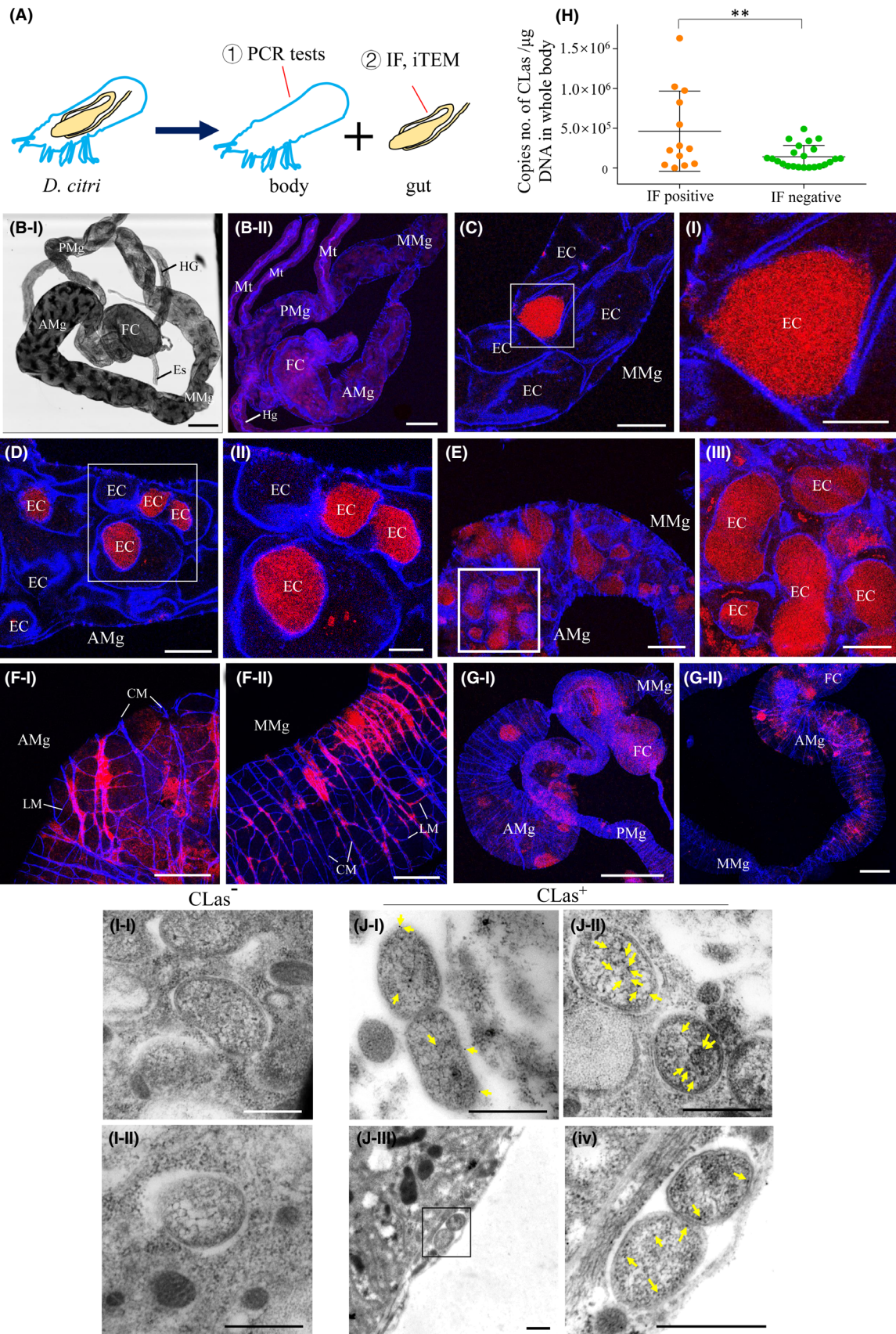
muscle, including circular muscle and longitudinal muscle (Fig. 5F). The CLas infection in circular muscle suggested that CLas may have traversed the basal lamina and reached the visceral muscle for accumulation (Fig. 5F). The CLas distribution in longitudinal muscle indicated that CLas moved along the muscle fibres to spread, ultimately infecting the whole alimentary canal (Fig. 5F and G). The tissue preference of CLas infection and distribution was not evident in these findings.

In addition, not all alimentary canal samples could be immunolabelled; only approximately 36.0% of alimentary canal samples were immunofluorescence-positive. CLas titres in *D. citri* bodies corresponding to immunofluorescence-positive and immunofluorescence-negative alimentary canal samples were analysed. The qPCR assay showed that the mean of CLas titres was 4.64×10^5 copies / μg insect DNA in *D. citri* bodies in which alimentary canal samples were immunofluorescence-positive. This finding was significantly higher than the titres from *D. citri* bodies in which alimentary canal samples were immunofluorescence-negative (Fig. 5H). Overall, when the CLas titre in the *D. citri* body was higher than 4.64×10^5 copies / μg DNA, the corresponding alimentary canal tended to be immunolabelled.

The iTEM showed that in alimentary canals of controls, abundant bacteria accumulated in epithelial cells, but OMP-333 could not be specifically immunolabelled (Fig. 5I). In the alimentary canal samples from CLas-positive bodies, OMP-333 specifically immunolabelled bacteria within epithelial cells (Fig. 5J–I and -II). OMP-333 also immunolabelled the bacteria in reticular tissues on the surface of the alimentary canal (Fig. 5J–III). These results are likely to record the process of CLas spread from epithelial cells to the outside of the alimentary canal.

Discussion

Recent studies on CLas have primarily focused on the identification of pathogens, improvement of the detection system and technique sensitivity, analysis of omics and preparation of antibodies (Ding *et al.*, 2015, 2016, 2017; Zheng *et al.*, 2016; Kruse *et al.*, 2017; Selvaraj *et al.*, 2018; Das *et al.*, 2019; Li *et al.*, 2021). The mechanisms underlying the interactions among CLas, citrus and *D. citri* have also gradually been revealed (Mann *et al.*, 2012, 2018; Ammar *et al.*, 2016; Ghanim *et al.*, 2016; Clark *et al.*, 2018; Wu *et al.*, 2018). The OMP, an important protein for bacterial structure, plays an important role in CLas infection and causes pathogenicity in plant hosts (Lin *et al.*, 2002). Investigation into OMP is beneficial for understanding the mechanisms of CLas pathogenicity, as well as the infection of CLas in the plant host and *D. citri* vectors. The development of antibodies against CLas OMP can be used for the establishment of targeted drug

systems and provides a strategy to control HLB occurrence and spread via neutralizing OMP.

Herein, the HLB occurrence in Fujian Province, China was surveyed. The symptomatic leaves were sampled and showed diverse positive rates of CLas. The CLas titres in the leaves of different citrus cultivars, including Tangelo (*C. paradisi*×*C. tangerine*) and *C. sinensis* var. *brasiliensis* Tanaka, sampled from different geographic areas, showed a positive association of CLas infection levels with symptoms. This result was similar to the report of CLas in periwinkle (*Catharanthus roseus*), in which leaves with weak symptoms contain a low concentration of CLas, while the leaves with strong symptoms contain high concentrations of CLas (Ding *et al.*, 2015). These CLas-positive data in the survey on the occurrence of HLB reveal the urgent need for a strategy to control HLB. Therefore, we focused on the preparation for specific antibodies against OMP and utilized the antibodies to study CLas infection. Antibodies against several synthesized peptides of OMP amino acid sequences were prepared and tested. Antibodies against four peptides could recognize prokaryotic expression of OMP protein. Among these antibodies, OMP-47, OMP-225 and OMP-333 specifically detected antigens in total proteins of CLas-infected leaves or *D. citri* vectors in western blot assays. OMP-225 or OMP-333 was used for immunofluorescence and iTEM assays to characterize the morphology of CLas and trace the CLas infection in citrus leaves and *D. citri* vectors. We found that immunolabelled CLas was round or oval and accumulated in sieve cells of midribs of citrus leaves and axile placenta of diseased fruit. CLas also locally infected the epithelial cells of *D. citri* vectors, or infected the epithelial cells, visceral muscles and reticular tissues. We hypothesize that the CLas that accumulated in the epithelial cells spread across the surface of the alimentary canal where it propagated, accumulating in visceral muscles or reticular tissues. This provides evidence for the circulation of CLas. It is hypothesized that the circulation of CLas in insect vectors is similar to the infection route of persistent propagative plant viruses in insect vectors. The probable CLas infection route is by the ingestion of citrus sap by the *D. citri* vector, accession of CLas in the oesophagus, followed by the invasion of epithelial cells at an undefined site where CLas propagation begins. Abundant CLas accumulated in the initially infected epithelial cells, some entered the neighbouring cells via intercellular junctions and some traversed basal lamina and reached visceral muscles. These muscle fibres, working as bridges, facilitated the CLas infection in the whole alimentary canal. A time course assay should be conducted in the future to further confirm these findings.

A previous study has also reported the infection of CLas in citrus plants and *D. citri* vectors via fluorescence

assays. For example, Ammar *et al.* (2011) used fluorescence *in situ* hybridization (FISH), of which probes are specific for 16S rDNA, in citrus leaves and *D. citri* organs to characterize the infection of CLas. Both Ammar *et al.* (2011) and this study verified the specific accumulation of CLas in the phloem of citrus plants. However, the CLas infection and accumulation in *D. citri* vectors were different. CLas was detected as quasi-spherical or pleiomorphic bodies or short thin rods in the organs of *D. citri* in the study by Ammar *et al.* (2011). In contrast, in this study, CLas was diffusely distributed throughout the cytoplasm of epithelial cells of alimentary canal and visceral muscles (Fig. 5). Detailed analyses, such as the FISH assay, are merited for our additional studies.

In this study, we performed western blot, immunofluorescence, and iTEM analyses to test the specificity of OMP antibodies. OMP-225 specifically immunolabelled the phloem of CLas-infected midribs, which was consistent with previous studies that showed that CLas is distributed in the phloem of the stem, the seed coat and the root, based on a direct tissue blot immunoassay (Ding *et al.*, 2015, 2016, 2017). In this study, a bacteria-like structure immunolabelled with OMP-333 in iTEM was also localized to the phloem of the midribs. CLas appeared round and oval, and the size of CLas was consistent with that previously reported (Shokrollah *et al.*, 2010; Mann *et al.*, 2011; Hilf *et al.*, 2013). It is well-documented that the round or oval CLas is too large to pass through the sieve tube pores and to move from cell to cell; thus, it become more rod-like or small enough to fit through the pores (Bove, 2006; Sechler *et al.*, 2009; Shokrollah *et al.*, 2010; Mann *et al.*, 2011; Hilf *et al.*, 2013). However, the rod-shaped bacteria-like structure is absent here. It is known that the CLas genome determines the shape of CLas. However, it is unknown whether the OMP, a membrane protein outside of the CLas bacterium, could affect the bacterial shape or whether some domains of OMP function in shape change or are related to movement. More studies are merited to determine the answers to these questions. For the antibodies, these results indicated that OMP-225 and OMP-333 were specific for the citrus plants in this study. More tests are required to determine the specificity of these antibodies for other citrus species and cultivars. Overall, we hope that these antibodies could show reliable specificity for stems, seed coats and roots of most citrus species, thus being beneficial for HLB detection.

Experimental procedures

Insects, plants and CLas

Uninfected *D. citri* individuals were collected from orange jessamine (*Murraya* Koenig ex Linn.) plants at Fujian

Agriculture and Forestry University in Fuzhou, Fujian Province, China. These female *D. citri* individuals first laid eggs on orange jessamine plants in the greenhouse, and the parents of *D. citri* were tested using PCR assays for the presence of CLas. The offspring of CLas-negative females were reared on orange jessamine plants for several generations at 25 ± 3°C in the laboratory. Diseased leaves, fruit and infected *D. citri* individuals were collected from citrus plants with typical HLB symptom in Fuqing, Shunchang and Gutian, Fujian Province, China.

The uninfected citrus plants (*C. reticulata Blanco* cv. Shatangju) and orange jessamine plants were maintained in a greenhouse at Fujian Agriculture and Forestry University separately from *D. citri*.

DNA Extraction from citrus plants and D. citri *individuals*

Dellaporta DNA minipreparation was performed (Weigel and Glazebrook, 2009). In brief, 0.2 g of midribs of citrus leaves, axile placenta of fruit, or *D. citri* individuals were collected and ground with liquid nitrogen. The Dellaporta solution, which contained 10 ml of 1 M Tris, 10 ml of 0.5 M EDTA, 10 ml of 5 M NaCl and 70 μl 14.2 M β-mercaptoethanol, plus 300 μl 20% SDS were added and vortexed for 2 min. Then the mixture was incubated at 65°C for 10 min, followed by the addition 160 μl 5 M KOAc and vortexing for 2 min. After centrifuging at 15 871 *g* for 10–15 min, the supernatant was transferred into a tube that contained half of the amount of cold isopropanol and vortexed for 2 min. After centrifuging at 15 871 *g* for 10 min, the supernatant was discarded and the pellet was washed with 500 μl of 70% ethanol. The pellet was centrifuged for 5 min and dried using a speed-vacuum for 2–3 min. The DNA pellet of leaf midribs or axile placenta was resuspended in 200 μl of water, whereas the DNA pellet of *D. citri* individuals was resuspended in 7 μl of water.

PCR and qPCR Detection

PCR detection and identification were performed by targeting 16s rDNA of CLas in samples using the primer pairs 5′-GCGCGTATGCAATACGAGCGGCA-3′ and 5′-GCCTCGCGACTTCGCAACCCAT-3′ (Jagoueix *et al.*, 1996). The thermocycling profile was as follows: 95°C for 3 min, 35 cycles of 95°C for 30 s, 55°C for 30 s and 72°C for 45 s, and a final extension at 72°C for 5 min. The PCR products were detected with electrophoresis of 1.0% agarose gels.

For the quantification of CLas in leaf and *D. citri* samples, a standard curve of OMP was first confirmed. Specifically, the concentration of the plasmid DNA with the OMP gene fragment was determined using the NanoDrop 1000. The copy number of the OMP gene in a 10-fold dilution

series of the plasmid was calculated using the following formula: (DNA amount × 6.022 × 10^{23})/(plasmid length × 1 × 10^9 × 650). Specific primers for OMP (forward primer 5'-GCCGATAAGCTGGA

AGGGAA-3' and reverse primer 5'- AGACACCCATCA TCCCGAGT-3') were used to analyse the diluted plasmids for their Ct value. The qPCR assays were performed using 2 × RealStar Green Fast Mixture (with RXOII) (GenStar) in the CFX96 touch system (Bio-Rad, USA). Based on the correlation of the logarithm of plasmid copy number to base 10 with the corresponding Ct value, the equation y = −3.2058x + 37.4 for leaf samples and y = −3.2058x + 37.4 for *D. citri* samples were generated, where x is the logarithm of plasmid copy number to base 10, y is the Ct value and R^2 = 0.9988. The CLas titres in *D. citri* bodies were then determined using the same system and program as that for plasmid DNA. Based on the Ct value of the DNA samples and the equation, the copy number of OMP, which was used to indicate the CLas genome copy number, was determined as the log of the copy number per microgram of insect DNA.

Bioinformatics analysis of OMP

The presence and location of signal peptide cleavage sites in amino acid sequences of OMP were predicted using SignalP 4.0 (Petersen *et al.*, 2011). The transmembrane helices in amino acid sequences of OMP were predicted using the TMHMM 2.0 server (Krogh *et al.*, 2001; Moller *et al.*, 2001). The hydrophilicity and antigenicity of amino acid sequences of OMP were analysed using the software DNAman (Lynnon Biosoft, San Ramon, CA, USA).

Antibodies

The anti-OMP polyclonal antibodies against MHKSTED-FRRIKRLL, PQEIKESSEKISKYF and RHREGDKIQQFGFR OMP peptides at regions of 1–15 aa, 316–330 aa and 763–776 aa, respectively, were prepared by Beijing Protein Innovation (Beijing, China), which is approved by the Beijing Municipal Science and Technology Commission, China. The anti-OMP polyclonal antibodies against VRRIEIRGATNVGK, ERPFVRVKTRINRD and LGADK-LEGNDSFWR OMP peptides, at regions of 47–61 aa, 333–347 aa and 724–738 aa, respectively, were prepared by the GenScript Biotech Corporation (Nanjing, China), which is approved by the Science Technology Department of Jiangsu Province, China. The anti-OMP polyclonal antibodies against SFGKTDVYSKERMS, GNLYNPQEIKESSEK and YGIPLRHREGDKIQ OMP peptides at 225-238-61 aa, 311–325 aa and 758–771aa, respectively, were prepared by the Wuxi FuYang Biotech Co. Ltd (Wuxi, China), which is approved by the Science Technology Department of Jiangsu Province, China.

Rabbits were separately immunized with these synthesized peptides four times to generate anti-OMP serum. IgG was isolated from the antisera via a protein A-Sepharose affinity column (Thermo Fisher Scientific, Waltham, MA, USA), and then eluted in phosphate-buffered saline (PBS).

IgGs of OMP-225 were directly conjugated to rhodamine (OMP-225-rhodamine) according to manufacturer's instructions (Thermo Fisher Scientific). Actin dye rhodamine-phalloidin was obtained from Thermo Fisher Scientific.

Prokaryotic expression of OMP

The OMP gene from the DNA of diseased citrus plants sampled from citrus-growing fields in Fuqing, Fujian Province, China, were PCR amplified. The PCR products were purified and engineered into a pEASY-Blunt E1 Expression vector (Transgen Biotech, Beijing, China) containing 6×His-Tag. The resulting E1-OMP plasmids were transformed into *Escherichia coli* strain Rosetta and OMP proteins were expressed in the presence of isopropyl-β-D-thiogalactopyranoside (IPTG) (Sigma-Aldrich, Shanghai, China) (1 mM). The cells were harvested and detected for the prokaryotic expression of OMP with Anti-6×His-Tag mouse monoclonal antibody (Sangong, Shanghai, China) using western blots.

Western blots

To confirm the specificity of antibodies against OMP peptides, the total proteins of prokaryotic-expressed OMP, midribs separated from CLas-infected or uninfected leaves and *D. citri* collected from infected citrus plants or uninfected *D. citri* maintained in the laboratory were extracted and processed for immunoblotting. The antibodies (1:1000 dilution in 7% non-fat dry milk with TBST) were used to probe the OMP antigens. Horseradish peroxidase-conjugated goat anti-rabbit secondary antibodies (Sangong, China; 1:10000 dilution in 7% non-fat dry milk with TBST) were used to immunoblot the primary antibodies. Finally, the blots were developed using Peirce ECL Western Blotting Substrate (Thermo Fisher Scientific, USA) and observed using an ImageQuant LAS4000 mini from GE (Fairfield, CT, USA).

Frozen sections of plants

The CLas-positive midrib, CLas-positive axile placentas of citrus fruit, CLas-negative midribs derived from leaves of citrus plants maintained in laboratory, or CLas-negative midribs derived from leaves of orange jessamine (*Murraya* Koenig ex Linn.) plant were collected. These plant samples were embedded with O.C.T. compound (Sakura), and then sectioned with a Shandon

Cryotome FSE (Thermo Scientific). The sections were ultimately treated for immunofluorescence assay.

Immunofluorescence microscopy

The plant sections were immunolabelled with OMP-225-rhodamine for 2 h, then observed using a Leica TCS SP5 inverted confocal microscope (Wetzlar, Germany). The alimentary canal of *D. citri* was fixed in 4% paraformaldehyde in PBS for 2 h and treated with 0.2% Triton X-100 in PBS for 1 h, as previously described (Chen *et al.*, 2019). The alimentary canal was then immunolabelled with OMP-225-rhodamine or actin dye phalloidin-Alexa Fluor 647 carboxylic acid (Thermo Fisher Scientific). The treated samples were examined with a Leica TCS SP5 inverted confocal microscope (Wetzlar).

iTEM

The midribs of citrus leaves, axile placenta of citrus fruit, or the *D. citri* alimentary canal were fixed, dehydrated, embedded and cut into ultrathin sections, as previously described (Chen *et al.*, 2019). Briefly, sections were successively immunolabelled with OMP-333 as the primary antibody and goat anti-rabbit IgG conjugated with 10-nm-diameter gold particles as the secondary antibody (Abcam, Shanghai, China). The treated sections were examined with the transmission electron microscope (H-7650; Hitachi, Tokyo, Japan).

Conflict of Interest

The authors declare that they have no conflict of interest.

References

Ammar, E.D., Ramos, J.E., Hall, D.G., Dawson, W.O., and Shatters, R.G. Jr (2016) Acquisition, replication and inoculation of *Candidatus* Liberibacter asiaticus following various acquisition periods on Huanglongbing-infected Citrus by nymphs and adults of the Asian Citrus psyllid. *PLoS One* **11:** e0159594.

Ammar, E.D., Shatters, R.G., and Hall, D.G. (2011) Localization of *Candidatus* Liberibacter asiaticus, associated with citrus huanglongbing disease, in its psyllid vector using fluorescence in situ hybridization. *J Phytopathol* **159:** 726–734.

Bastianel, C., Garnier-Semancik, M., Renaudin, J., Bove, J.M., and Eveillard, S. (2005) Diversity of "*Candidatus* Liberibacter asiaticus," based on the omp gene sequence. *Appl Environ Microbiol* **71:** 6473–6478.

Bishop, R.E. (2008) Structural biology of membrane-intrinsic beta-barrel enzymes: sentinels of the bacterial outer membrane. *Biochim Biophys Acta* **1778:** 1881–1896.

Bove, J.M. (2006) Huanglongbing: a destructive, newly-emerging, century-old disease of citrus. *J Plant Pathol* **88,** 7–37.

Chen, Q., Godfrey, K., Liu, J., Mao, Q., Kuo, Y.W., and Falk, B.W. (2019) A Nonstructural protein responsible for viral spread of a novel insect reovirus provides a safe channel for biparental virus transmission to progeny. *J Virol* **93:** e00702–e719.

Clark, K., Franco, J.Y., Schwizer, S., Pang, Z., Hawara, E., Liebrand, T.W.H., *et al.* (2018) An effector from the Huanglongbing-associated pathogen targets citrus proteases. *Nat Commun* **9:** 1718.

Dala-Paula, B.M., Plotto, A., Bai, J., Manthey, J.A., Baldwin, E.A., Ferrarezi, R.S., and Gloria, M.B.A. (2018) Effect of huanglongbing or greening disease on orange juice quality, a review. *Front Plant Sci* **9:** 1976.

Das, A.K., Nerkar, S., Gawande, N., Thakre, N., and Kumar, A. (2019) SCAR marker for Phytophtora nicotianae and a multiplex PCR assay for simultaneous detection of P. nicotianae and *Candidatus* Liberibacter asiaticus in citrus. *J Appl Microbiol* **127:** 1172–1183.

Ding, F., Duan, Y., Paul, C., Brlansky, R.H., and Hartung, J.S. (2015) Localization and distribution of '*Candidatus* Liberibacter asiaticus' in Citrus and Periwinkle by direct tissue blot immuno assay with an anti-OmpA polyclonal antibody. *PLoS One* **10:** e0123939.

Ding, F., Duan, Y., Yuan, Q., Shao, J., and Hartung, J.S. (2016) Serological detection of '*Candidatus* Liberibacter asiaticus' in citrus, and identification by GeLC-MS/MS of a chaperone protein responding to cellular pathogens. *Sci Rep* **6:** 29272.

Ding, F., Paul, C., Brlansky, R., and Hartung, J.S. (2017) Immune tissue print and immune capture-PCR for diagnosis and detection of *Candidatus* Liberibacter Asiaticus. *Sci Rep* **7:** 46467.

Ghanim, M., Fattah-Hosseini, S., Levy, A., and Cilia, M. (2016) Morphological abnormalities and cell death in the Asian citrus psyllid (*Diaphorina citri*) midgut associated with *Candidatus* Liberibacter asiaticus. *Sci Rep* **6:** 33418.

Gottwald, T.R. (2010) Current epidemiological understanding of citrus Huanglongbing. *Annu Rev Phytopathol* **48:** 119–139.

Grafton-Cardwell, E.E., Stelinski, L.L., and Stansly, P.A. (2013) Biology and management of Asian citrus psyllid, vector of the huanglongbing pathogens. *Ann Rev Entomol* **58:** 413–432.

Halbert, S.E., and Manjunath, K.L. (2004) Asian citrus psyllids (Sternorrhyncha: Psyllidae) and greening disease of

citus: a literature review and assessment of risk in Florida. *Fla Entomol* **87:** 330–353.

Hilf, M.E., Sims, K.R., Folimonova, S.Y., and Achor, D.S. (2013) Visualization of 'candidatus liberibacter asiaticus' cells in the vascular bundle of citrus seed coats with fluorescence in situ hybridization and transmission electron microscopy. *Phytopathology* **103:** 545–554.

Hocquellet, A., Toorawa, P., Bove, J.M., and Garnier, M. (1999) Detection and identification of the two *Candidatus* Liberobacter species associated with citrus huanglongbing by PCR amplification of ribosomal protein genes of the beta operon. *Mol Cell Probes* **13:** 373–379.

Hung, T.H., Hung, S.C., Chen, C.N., Hsu, M.H., and Su, H.J. (2004) Detection by PCR of *Candidatus* Liberibacter asiaticus, the bacterium causing citrus huanglongbing in vector psyllids: application to the study of vector-pathogen relationships. *Plant Pathol* **53:** 96–102.

Jagoueix, S., Bove, J.M., and Garnier, M. (1996) PCR detection of the two 'Candidatus' Liberobacter species associated with greening disease of citrus. *Mol Cell Probes* **10:** 43–50.

Jagoueix, S., Bove, J.M., and Garnier, M. (1997) Comparison of the 16S/23S ribosomal intergenic regions of "Candidatus Liberobacter asiaticum" and "Candidatus Liberobacter africanum," the two species associated with citrus huanglongbing (greening) disease. *Int J Syst Bacteriol* **47:** 224–227.

Krogh, A., Larsson, B., von Heijne, G., and Sonnhammer, E.L. (2001) Predicting transmembrane protein topology with a hidden Markov model: application to complete genomes. *J Mol Biol* **305:** 567–580.

Kruse, A., Fattah-Hosseini, S., Saha, S., Johnson, R., Warwick, E.R., Sturgeon, K., *et al.* (2017) Combining 'omics and microscopy to visualize interactions between the Asian citrus psyllid vector and the Huanglongbing pathogen *Candidatus* Liberibacter asiaticus in the insect gut. *PLoS One* **12:** e0179531.

Li, T., Zhang, L., Deng, Y., Deng, X., and Zheng, Z. (2021) Establishment of a Cuscuta campestris-mediated enrichment system for genomic and transcriptomic analyses of 'Candidatus Liberibacter asiaticus'. *Microb Biotechnol* **14:** 737–751.

Lin, J., Huang, S., and Zhang, Q. (2002) Outer membrane proteins: key players for bacterial adaptation in host niches. *Microbes Infect* **4:** 325–331.

Mann, M., Fattah-Hosseini, S., Ammar, E.-D., Stange, R., Warrick, E.R., Sturgeon, K., *et al.* (2018) Diaphorina citri nymphs Are resistant to morphological changes induced by "Candidatus Liberibacter asiaticus" in midgut epithelial cells. *Infect Immun* **86.**

Mann, R.S., Ali, J.G., Hermann, S.L., Tiwari, S., Pelz-Stelinski, K.S., Alborn, H.T., and Stelinski, L.L. (2012) Induced release of a plant-defense volatile 'deceptively' attracts insect vectors to plants infected with a bacterial pathogen. *PLoS Pathog* **8:** e1002610.

Mann, R.S., Pelz-Stelinski, K., Hermann, S.L., Tiwari, S., and Stelinski, L.L. (2011) Sexual transmission of a plant pathogenic bacterium, *Candidatus* Liberibacter asiaticus, between conspecific insect vectors during mating. *PLoS One* **6:** e29197.

Merfa, M.V., Perez-Lopez, E., Naranjo, E., Jain, M., Gabriel, D.W., and De La Fuente, L. (2019) Progress and obstacles in culturing 'Candidatus liberibacter asiaticus', the bacterium associated with Huanglongbing. *Phytopathology* **109:** 1092–1101.

Moller, S., Croning, M.D., and Apweiler, R. (2001) Evaluation of methods for the prediction of membrane spanning regions. *Bioinformatics* **17,** 646–653.

Parker, J.K., Wisotsky, S.R., Johnson, E.G., Hijaz, F.M., and Fuente, L.D.L. (2014) Viability of 'Candidatus Liberibacter asiaticus' prolonged by addition of citrus juice to culture medium. *Phytopathology* **104:** 15–26.

Petersen, T.N., Brunak, S., von Heijne, G., and Nielsen, H. (2011) Signalp 4.0: discriminating signal peptides from transmembrane regions. *Nat Methods* **8:** 785–786.

Sagaram, U.S., DeAngelis, K.M., Trivedi, P., Andersen, G.L., Lu, S.E., and Wang, N. (2009) Bacterial diversity analysis of Huanglongbing pathogen-infected citrus, using PhyloChip arrays and 16S rRNA gene clone library sequencing. *Appl Environ Microbiol* **75:** 1566–1574.

Sechler, A., Schuenzel, E.L., Cooke, P., Donnua, S., Thaveechai, N., Postnicova, E., *et al.* (2009) Cultivation of 'Candidatus Liberibacter asiaticus', 'Ca. L. africanus', and 'Ca. L. americanus' associated with Huanglongbing. *Phytopathology* **99:** 480–486.

Selvaraj, V., Maheshwari, Y., Hajeri, S., Chen, J., McCollum, T.G., and Yokomi, R. (2018) Development of a duplex droplet digital PCR assay for absolute quantitative detection of "Candidatus Liberibacter asiaticus". *PLoS One* **13:** e0197184.

Shokrollah, H., Abdullah, T.L., Sijam, K., Nor, S., and Abdullah, A. (2010) Ultrastructures of *Candidatus* Liberibacter asiaticus and its damage in huanglongbing (hlb) infected citrus. *Afr J Biotechnol* **9:** 5897–5901.

Weigel, D., and Glazebrook, J. (2009) Dellaporta miniprep for plant DNA isolation. *Cold Spring Harbor Protocols* **2009:** pdb prot5178.

Wu, F., Huang, J., Xu, M., Fox, E.G.P., Beattie, G.A.C., Holford, P., *et al.* (2018) Host and environmental factors influencing 'Candidatus Liberibacter asiaticus' acquisition in Diaphorina citri. *Pest Manag Sci* **74:** 2738–2746.

Zheng, Z., Chen, J., and Deng, X. (2018) Historical perspectives, management, and current research of Citrus HLB in Guangdong province of China, where the disease has been endemic for over a hundred years. *Phytopathology* **108:** 1224–1236.

Zheng, Z., Xu, M., Bao, M., Wu, F., Chen, J., and Deng, X. (2016) Unusual five copies and dual forms of nrdB in "Candidatus Liberibacter asiaticus": biological implications and PCR detection Application. *Sci Rep* **6:** 39020.

Supporting information

Additional supporting information may be found online in the Supporting Information section at the end of the article.

Fig. S1. Prediction of the signal peptide (A) and hydrophobic regions (B) for OMP generated using SignalP 4.0 and TMHMM, respectively.

Table S1. CLas titres in the symptomatic and asymptomatic leaves of symptomatic or asymptomatic plants of Tangelo (*C. paradisi*×*C. tangerine*) and *C. sinensis* var. *brasiliensis* Tanaka.